Characteristics of diurnal variability at the ocean surface: spatial/temporal distribution from data and models

Supported By: NASA's Earth Science Division: Drs. Eric Lindstrom and Martha Maiden

Remote Sensing Systems
www.remss.com

Chelle L. Gentemann, Remote Sensing Systems, gentemann@remss.com

Several recent studies have concluded that coupled climate models should utilize a diurnally varying SST to examine the details of the boundary layer response and ensuing air-sea interactions. The global distribution of diurnal warming is clearly linked to wind speed and will therefore respond to the climatic distributions and seasonal or anomalous changes in wind speed, as shown by the response to ENSO wind speed anomalies. The Subtropical High regions in each ocean basin, and the Tropical Indian and Western Pacific Oceans have the largest averages of diurnal warming. The intra-day variability of surface warming has been related to the stability of the boundary layer and atmospheric convection. Since the tropical convection is an important driver of global atmospheric circulation, this example of ocean-atmospheric feedback underscores how diurnal warming of the ocean surface may influence larger scale weather patterns and climate. Results from several satellites show significant diurnal warming present over large regions. Several models (both empirical and physical) of diurnal variability have been developed, but show little agreement with each other. Comparisons of data and models will be used to discuss the global spatial/temporal distribution of diurnal warming and how accurately we actually understand it.

1. Characteristics of diurnal warming from observations and a model

Using data from 2002-2010, the observed mean and maximum diurnal warming is shown in Figures 1 and 2. Figure 1 shows AMSR-E (A) diurnal warming to be less than MODIS (B). The CG04 model (C) agrees well with AMSR-E primarily because it was developed using microwave SST data from TMI. While there is significant, extensive warming in the tropical Western Pacific and Indian oceans, there is also considerable warming in the midlatitude low wind regions. There are large day-night differences in MODIS at high latitudes that are likely not diurnal warming. Figure 2 shows the maximum diurnal warming, showing warming events of ~5 C in the Equatorial cold tongue, and midlatitude low wind regions. Although the mean diurnal warming is not large in the mid-latitude regions, it is important to recognize that these regions have large, but sporadic warming events. The model (Figure 2C) does not capture the large events well.

These results show the difficulty in understanding diurnal warming. The warming measured depends on instrument, spatial resolution, time of observation, depth of observation. The warming modeled depends on model utilized and data inputs. It is likely that there is no single answer for how to model diurnal warming, but instead, a different answer for each specific question. To remove diurnal warming from observations and calculate a 'foundation' or diurnally-corrected SST, it may be best to use a model developed from the observations themselves. To model warming for input into a climate model, it is necessary to understand whether a skin or 1-m model of diurnal amplitudes is desired and what the spatial resolution of the model is.

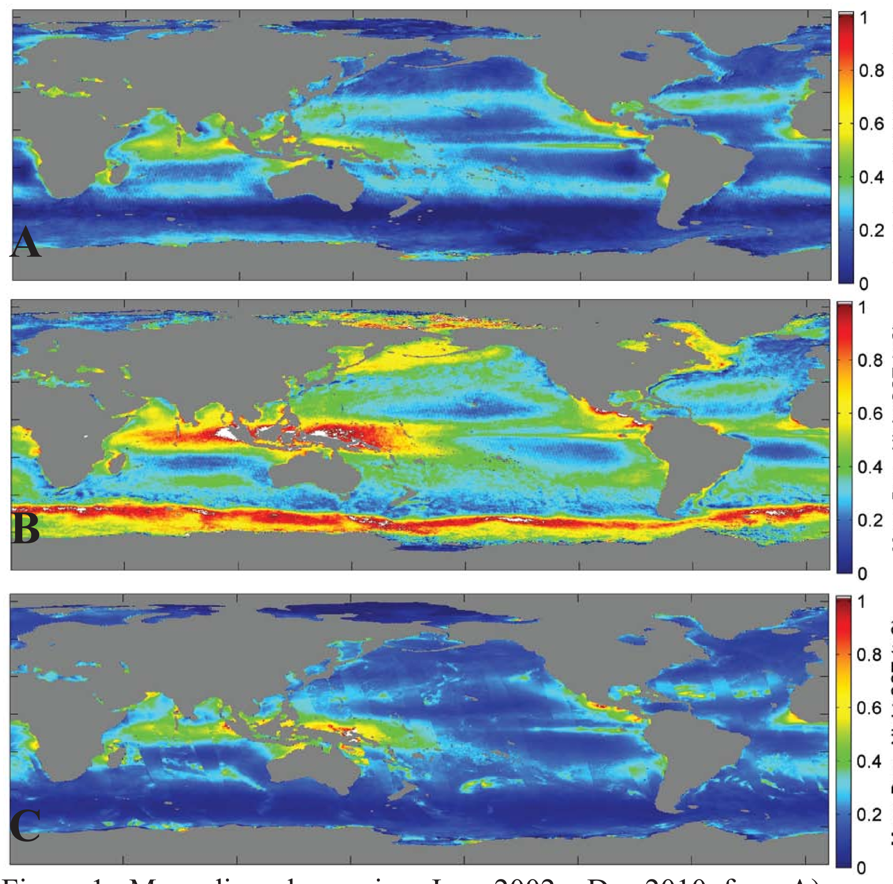

Figure 1. Mean diurnal warming, June 2002 – Dec 2010, from A) AQUA AMSR-E, B) AQUA MODIS, and C) CG04 model. The mean diurnal warming for was calculated by subtracting a 5-day nighttime average from daily daytime (2PM) data. The AMSR-E and MODIS instruments are both carried on the AQUA satellite which has a 2PM Local-Equatorial-Crossover-Time.

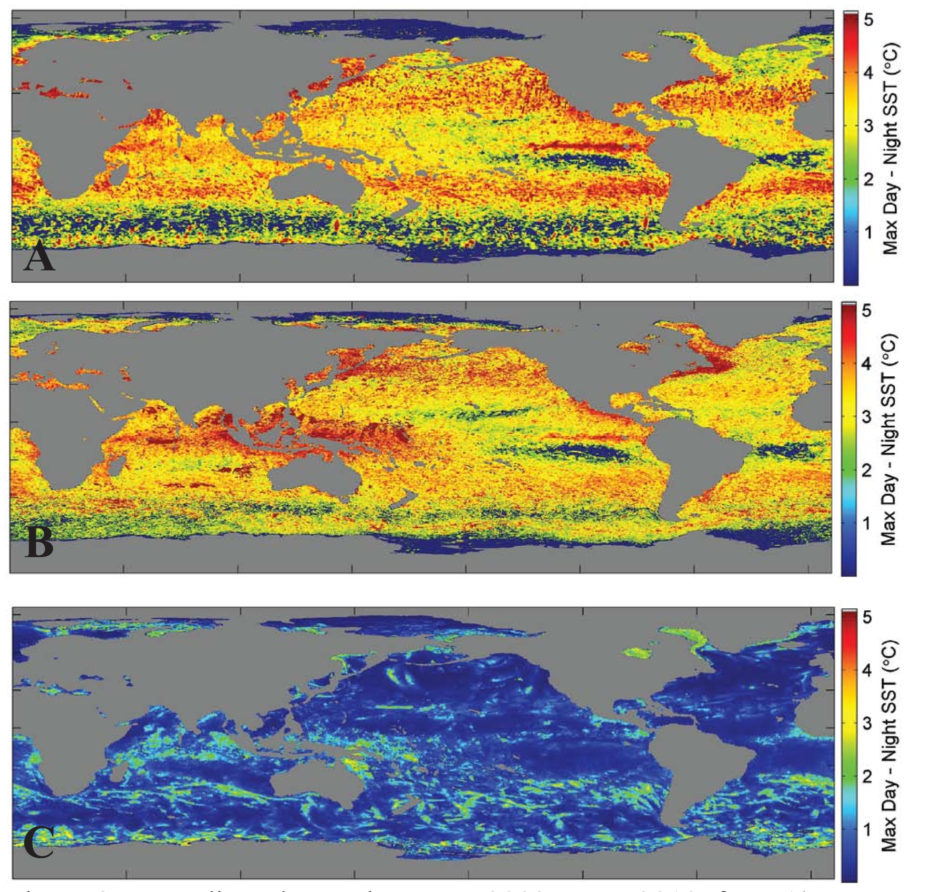

Figure 2. Max diurnal warming, June 2002 – Dec 2010, from A) AQUA AMSR-E, B) AQUA MODIS, and C) CG04 model. The max diurnal warming for was calculated by subtracting a 5-day nighttime average from daily daytime (2PM) data. The maximum difference, when wind speeds were less than 2 m/s, was saved. This is to illustrate where large diurnal events occur and compare the data results to model results.

2. Characteristics of diurnal warming from several models

A number of recently published papers (Kawai and Kawamura, 2004; Olsen et al., 2004; Stuart-Menteth et al., 2004; Weitlich, 2005; Kawai et al., 2006; Clayson and Weitlich, 2007) examine the spatial and temporal variability of diurnal warming, the impact of diurnal warming on air-sea heat and gas fluxes, and the impact of diurnal warming on regional weather patterns. The sensitivity studies for several models revealed significant differences between the models, prompting a study on the global distributions of diurnal warming from different models. Table 1 gives a summary of each model. As expected, the different models result in very different global distributions of diurnal warming. Using the ECMWF 40-year reanalysis monthly mean data sets from 1957 – 2002, total cloud fraction, wind speed, and surface solar radiation were averaged into a single climatological field for each variable. These climatologies were then used in each diurnal model to calculate the global distribution of diurnal warming (Figure 1). The L91 model is very different in spatial distribution of warming and magnitudes, mainly due to the 0.75 K minimum warming implicit in the model. The peak warming appears along the low wind regions in the mid-latitudes, but almost no warming appears in the tropics because the model is not driven by solar forcing. The W96, KK02, KK03, CG04, and ASM models all have somewhat similar distributions of warming with maxima in the low wind mid-latitude regions and a second maximum in the tropical western Pacific and Indian Oceans. The W96 and KK02 models have the largest amplitudes, then the ASM model, and the smallest amplitudes are seen in the CG04 model.

Table 1. Summary of empirical diurnal models

Model	Inputs	Output	Max (K)	Min (K)
L91	$u\ C_f$	DW_{peak}	2.4	0.75
W96	$u_{av}\ Q_{max}\ P$	DW_{peak}	2.4	-0.30
KK02 skin	$u_{av}\ Q_{max}$	DW_{peak}	13.5	0.0
KK02 bulk	$u_{av}\ Q_{max}$	DW_{peak}	2.8	0.0
CG04	$U_{inst}\ Q_{av}$	DW(t)	2.8	0.0
ASM sub-skin	$u_{0\text{-}6}\ u_{8\text{-}12}\ u_{12\text{-}15}\ u_{16\text{-}24}\ Q_{6\text{-}12}\ Q_{12\text{-}18}$	DW(t)	14.5	0.0
ASM bulk	$u_{0\text{-}6}\ u_{8\text{-}12}\ u_{12\text{-}15}\ u_{16\text{-}24}\ Q_{6\text{-}12}\ Q_{12\text{-}18}$	DW(t)	4.0	0.0

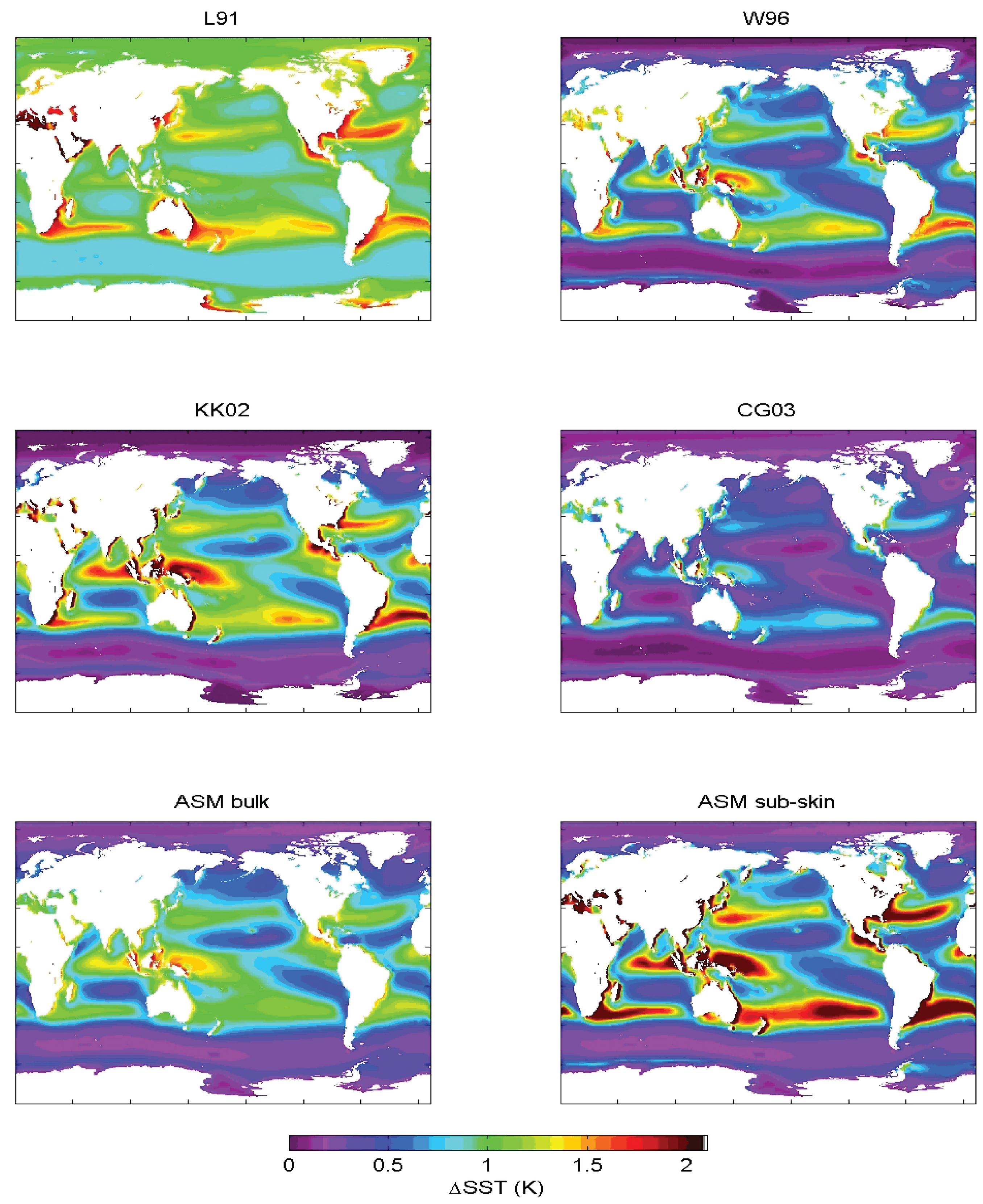

Figure 1. Global distribution of diurnal warming, using ECMWF 40-year climatology as inputs for each model. L91 = Lukas (1991), W96 = Webster et al. (1996), KK02 = Kawai and Kawamura (2002), CG04 = Gentemann (2003), updated, ASM bulk = Stuart-Menteth et al., 2004, ASM skin = Stuart-Menteth et al., 2004

3. Characteristics of extreme diurnal warming events (>5 C)

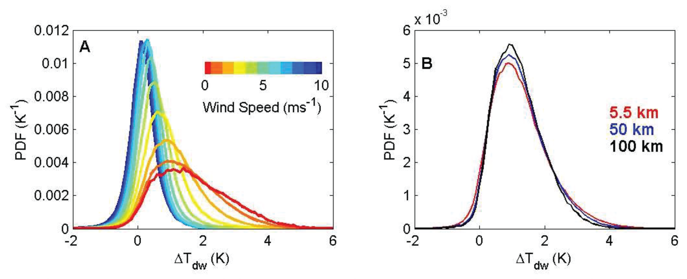

Figure 1. A) PDF of the SEVIRI day (14:00 LMT) minus night SST difference, ΔTdw, for different wind speeds. B) PDF of ΔTdw for wind speeds <3 ms-1 at different spatial resolutions. As averaging increases, the probability of diurnal events <2 K increases while the probability of larger diurnal events decreases.

The Probability Density Functions (PDFs) of SEVIRI ΔTdw at 14:00 LMT for (A) different wind speeds and (B) after averaging to different spatial resolutions are shown in Figure 1. Figure 1A shows that low wind speeds are associated with significant diurnal warming. The distribution peak shifts towards zero and narrows as wind speeds increase. The lowest wind speed class (<1ms-1) has the highest probability of diurnal events over 1.0 K (60.2%), with the probability of large events decreasing smoothly with increasing wind speed. Although not common, the figure clearly demonstrates that events over 4 K occur. The probability of a diurnal warming event larger than 5 K is 0.5%, 4 K is 3.5%, and 3 K is 14.6% at wind speeds less than 1 ms-1. Variability in diurnal warming is directly related to wind speed, variability in insolation, and variability in wind speed prior to 14:00 LMT SEVIRI measurement. The larger diurnal events likely had low wind speeds for several hours prior to 14:00 LMT, while the smaller diurnal events may have had higher or more variable wind speeds. Figure 1B shows the effect of spatial resolution on the probability of diurnal warming, for wind speeds less than 3 ms-1. As the spatial resolution decreases, the probability of diurnal heating > 2 K decreases, while the probability of smaller diurnal events, < 2 K, increases. The effect is largest for the lowest spatial resolution. These results clearly demonstrate that spatial resolution will affect measurement of diurnal warming. In the next section several diurnal events are studied using satellite measurements of diurnal warming at different spatial resolutions.

Diurnal warming events between 5 and 7 K, spatially coherent over large areas (~1000 km), are observed in independent satellite measurements of ocean surface temperature. The majority of the large events occurred in the extra-tropics. Given sufficient heating (from solar radiation), the location and magnitude of these events appears to be primarily determined by large-scale wind patterns. The amplitude of the measured diurnal heating scales inversely with the spatial resolution of the different sensors used in this study. These results indicate that predictions of peak diurnal warming using wind speeds with a 25 km spatial resolution available from satellite sensors and those with 50-100 km resolution from Numerical Weather Prediction models may have underestimated warming. Thus, the use of these winds in modeling diurnal effects will be limited in accuracy by both the temporal and spatial resolution of the wind fields. Failure to account for a diurnal cycle in sea surface temperatures (SSTs) can lead to errors in determining surface fluxes for Numerical Weather Prediction (NWP) and climate models (Webster et al., 1996; Woods et al., 1984). These large diurnal events are not well reproduced by any existing physical or empirical model.

Three independent satellite datasets were used to investigate large diurnal warming events. The AQUA satellite carries both the Advanced Microwave Scanning Radiometer - Earth Observing System (AMSR-E) and the Moderate Resolution Imaging Spectroradiometer (MODIS), providing independent contemporaneous microwave (MW) and infrared (IR) measurements. The AQUA satellite was launched in May 2002 into a polar, sun-synchronous orbit, with a LECT (Local Equator Crossing Time) of 1:30 AM/PM. Over much of the Atlantic Ocean, the geostationary METEOSAT-8 Second Generation (MSG) Spinning Enhanced Visible and Infrared Imager (SEVIRI) provides hourly data. While both MODIS and SEVIRI measure IR radiances, the SEVIRI instrument and viewing geometry is different than MODIS and is therefore independent.

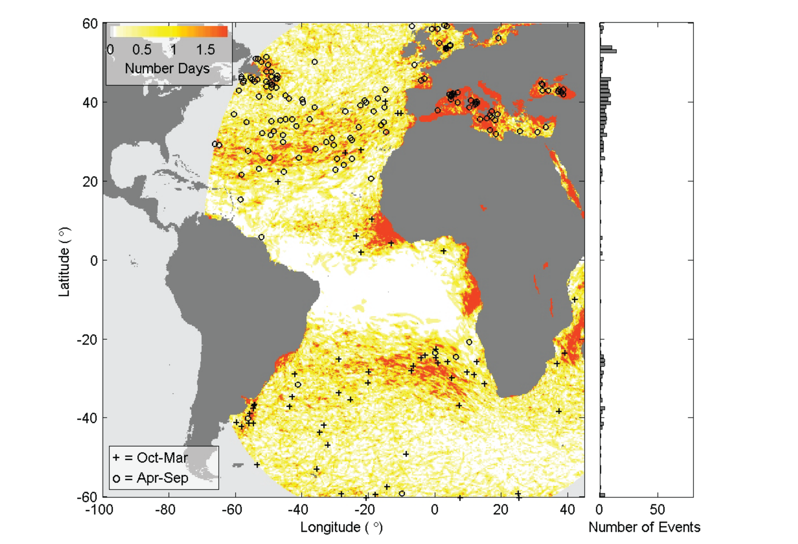

Figure 2. Location of diurnal events over 5 K (black '+' and 'o'). Events generally occur in the boreal(austral) summer. The background color shows the days in a year (on average) that wind speed was < 1 ms-1 at 14:00 LMT.

The SEVIRI day-night differences were examined for spatially coherent large positive differences over 5 K. 595 events were found (Figure 2). Low wind speeds occur more frequently where large diurnal warm events were also found, except in the Tropics where two regions off Africa show frequent low winds, but no large events. Near Angola, cloud cover prevented retrieval of IR SSTs during low wind events. The West African area is known to have aerosol biasing (which cools the IR SSTs) and this may have masked and reduced large warming events. Images of the daily diurnal events are available as auxiliary materials . Once these large events were identified in the SEVIRI data, verification using other sensors was completed.

These measurements by independent sensors reveal that large diurnal warming events at the ocean surface occur (with peaks > 5 K) more frequently then previously thought. The maximum warming measured depended on the spatial resolution of the sensor, but generally the three sensors showed remarkable agreement. Almost all large diurnal events occurred where low wind speeds occur, at latitudes outside 20° S to 20° N. There are several regions where low wind speeds are common in the Tropics, but no large events were found. Tropical SSTs rarely increase above 30°C and there may be a physical mechanism to limit large diurnal events. Studies have explored why Tropical SSTs seldom surpass 30°C (see review in Webster et al. (1996)), focusing on nonlinear feedback mechanisms between SST variability and clouds. However, for much of the equatorial Atlantic, Figure 2 indicates that the absence of large diurnal events is because of a lack of very low (< 1 ms-1) wind speeds. To ensure that absence of large diurnal events is not due to IR sampling (clouds preventing measurement) or algorithm errors (an underestimation of warming due to high vapor amounts), AMSR-E SSTs were similarly analyzed for large diurnal events (see auxiliary materials1). The MW SSTs are able to measure through clouds, are not biased by water vapor. They confirm the absence of large diurnal events in the Tropics.

4. Air-Sea interactions: Diurnal warming and ENSO

Diurnal models all depend strongly on wind speed. At low wind speeds, small changes in wind speed will result in a large change in diurnal warming amplitudes. To illustrate this, this we chose a location in the Equatorial Cold Tongue where the wind speed is strongly controlled by the stability of the boundary layer and SST (Chelton et al., 2001). Using a time series of SSM/I wind speeds, we calculated daily diurnal warming at 2 PM (the peak value for CG04 model). The Multivariate ENSO Index (MEI) (Wolter and Timlin, 1993; Wolter and Timlin, 1998) is a measure of the strength and timing of ENSO events. Figure 5 shows the MEI in the background (El Niño in yellow/red and La Niña in blues). The CG04 modeled diurnal warming is shown by the blue line. The heavy black lines is a least-squares estimate of the diurnal warming annual/biannual magnitude.

This fit to the diurnal amplitudes was completed to allow for comparison of the usual diurnal warming modeled, versus the warming during ENSO. In non-ENSO years, there is normally a cold tongue of water in the Eastern Pacific and the wind speeds are close to their climatological value. During the El Niño the Equatorial Pacific warms and the equatorial cold tongue is suppressed by the surge of warm water from the western Pacific and the wind speeds in the Eastern Pacific are larger than their climatological value.

Conversely, during a La Niña the cold tongue is larger than normal and the wind speeds are less than their climatological value. The cold tongue influences the wind speed (Figure 1) by increasing the stability of the boundary layer and thereby decreasing the vertical transfer of momentum (Chelton et al., 2001). The cold tongue is clearly seen in both the SST and the surface wind stress.

Figure 2 shows that during the El Niño phase, the diurnal warming is significantly less than usual during the winter. The warmer ocean temperatures during the El Niño, result in higher wind speeds and less diurnal warming than seen during ENSO neutral years such as 1996. The large 1998 El Niño resulted in a less diurnal warming than previous years. Conversely, during the 1999-2000 La Niña there is more diurnal warming as the strong cold tongue present decreases wind speeds.

The impact of large-scale atmospheric events, such as ENSO, on SST and wind speed is shown to impact the surface diurnal warming, which can then affect the air-sea heat fluxes. These types of feedbacks would be best studied through coupled models that resolve diurnal SST variability.

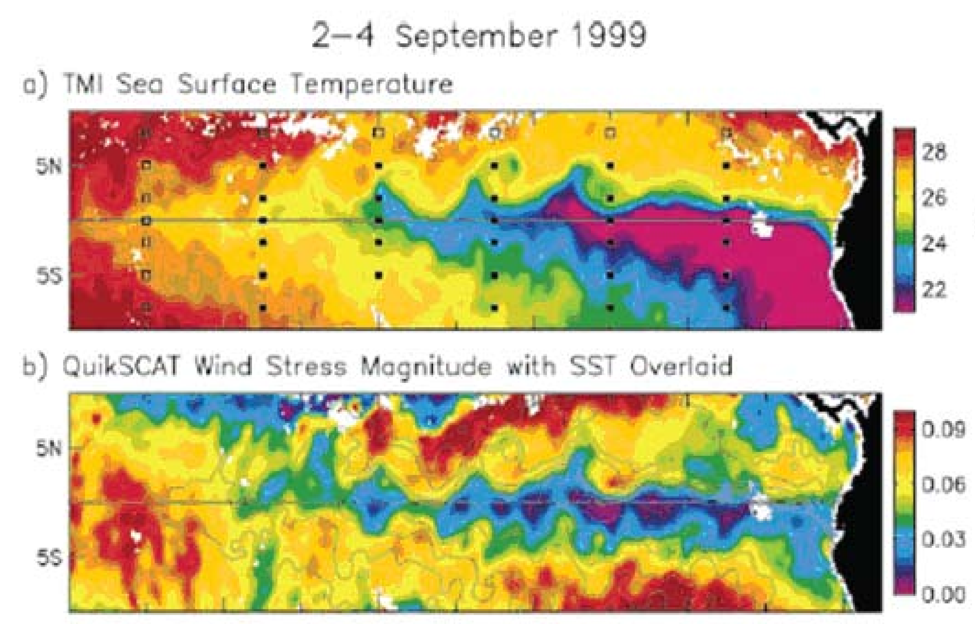

Figure 2. Figure illustrating the influence of the equatorial cold tongue on surface wind speeds. The figure shows a 3-day average, from 2-4 September 1999, of a) TMI sea surface temperature and b) QuikSCAT wind stress magnitude with SST overlaid. Figure from (Chelton et al., 2001).

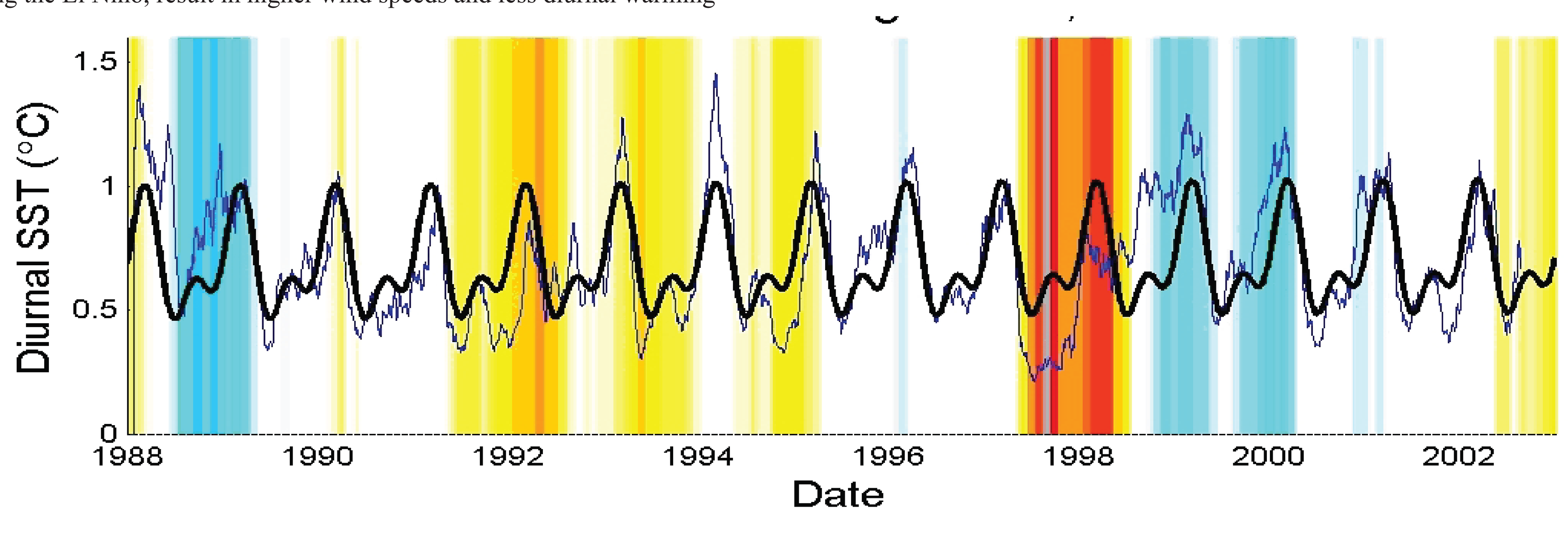

Figure 2. Maximum diurnal warming at 80°W, 0°N modeled by the CG04 diurnal model. This time series of diurnal warming is located in the Equatorial Cold Tongue. The background color is the MEI, red/yellow is for El Niño and blue for La Niña. The thin blue line shows the CG04 model estimate of diurnal warming using SSM/I wind speeds. The thick black line is a fit to the mean annual cycle in diurnal warming.